Dynamics of Solitary-waves in the Coupled Korteweg-De Vries Equations

Woo-Pyo Hong and Jong-Jae Kim

Department of Physics, Catholic University of Daegu, Hayang, Kyongsan, Kyungbuk 712-702, South Korea

Reprint requests to Dr. W.-P. H.; E-mail: wphong@cu.ac.kr

Z. Naturforsch. **60a,** 557 – 565 (2005); received February 14, 2005

We find new analytic solitary-wave solutions, having a nonzero background at infinity, of the coupled Korteweg-De Vries equation, using the auxiliary function method. We study the dynamical properties of the solitary-waves by numerical simulations. It is shown that the solitary-waves can be stable or unstable, depending on the coefficients of the model. We study the interaction dynamics by using the solitary-waves as initial profiles to show that the mass and energy of the coupled Korteweg-De Vries can be conserved for a negative third-order dispersion term. — PACS numbers: 03.40.Kf, 02.30.Jr, 47.20.Ky, 52.35.Mw

Key words: Coupled Korteweg-De Vries Equations; Analytic Solitary-wave Solutions; Numerical Simulations; Stability; Interaction.

1. Introduction

In this paper, we consider a system of the coupled Korteweg-De Vries (cKdV) equations

$$\begin{aligned} &u_t + \alpha v v_x + \beta u u_x + \gamma u_{xxx} = 0, \\ &v_t + \delta (uv)_x + \varepsilon v v_x = 0, \end{aligned} \tag{1}$$

where α, β, δ, and ε are all nonzero constant, related to a physical situation [1 – 3]. Here, $\alpha v v_x$ acts as a force term on the first Korteweg-De Vries (KdV) equation, which is coupled to the second equation of similar type, but, without any dispersion term. The cKdV type equations have been widely studied in fields of physical and engineering sciences such as nonlinear optics, superconductors, plasmas, fluid dynamics and supersymmetry [4, 5]. Several solitary-wave solutions of the cKdV equation have been found in [1, 2]. More recently, Tian and Gao [3] have reported some exact analytic solitary-wave solutions of (1), using an auto-Bäcklund transformation.

The purpose of this paper is to find new analytic solitary-wave solutions of (1) by using the auxiliary differential equation method [6, 7] and investigate their dynamical behavior. In Section 2 we introduce the auxiliary differential equation method for finding solitary-wave solutions and perform symbolic computations. In Section 3 we investigate the dynamics of the solitary-waves and their interactions by a numerical method. The conclusions are in Section 4.

2. The Auxiliary Equation Method and Analytic Solitary-wave Solutions

In this section, we first describe the auxiliary equation method [6, 7]. Suppose we are given coupled nonlinear partial differential equations (NLPDE) for $u(x,t)$ and $v(x,t)$ in the form

$$\begin{aligned} &H_1(u, v, u_x, v_x, u_t, v_t, u_{xx}, v_{xx}, u_{tt}, v_{tt}, u_{xt}, v_{xt} \ldots) = 0, \\ &H_2(u, v, u_x, v_x, u_t, v_t, u_{xx}, v_{xx}, u_{tt}, v_{tt}, u_{xt}, v_{xt} \ldots) = 0. \end{aligned} \tag{2}$$

Introducing the similarity variable $\xi = kx - \omega t$, the traveling wave solutions of $u(\xi)$ and $v(\xi)$ satisfy the ODEs

$$\begin{aligned} &G_1(u, v, u_\xi, v_\xi, u_{\xi\xi}, v_{\xi\xi}, u_{\xi\xi\xi}, v_{\xi\xi\xi}, \ldots) = 0, \\ &G_2(u, v, u_\xi, v_\xi, u_{\xi\xi}, v_{\xi\xi}, u_{\xi\xi\xi}, v_{\xi\xi\xi}, \ldots) = 0. \end{aligned} \tag{3}$$

We seek the solution of (3) in the forms

$$u(\xi) = \sum_{i=0}^{n} u_i z^i(\xi), \quad v(\xi) = \sum_{j=0}^{m} v_j z^j(\xi), \tag{4}$$

where u_i ($i = 1, 2, ..., n$) and v_i ($j = 1, 2, \ldots, m$) are all real constants to be determined, the orders m and n are positive integers which can be readily determined by balancing the highest order derivative term with the highest power nonlinear term in (3). The main point of the present method is to introduce $z(\xi)$ as the solutions

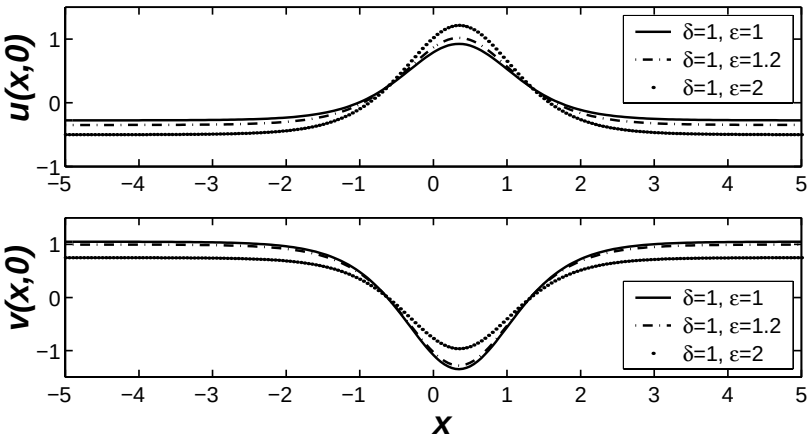

Fig. 1. The profiles of bright and dark solitary-waves $u(x,0)$ and $v(x,0)$, respectively. The parameters a, b, and c satisfy the auxiliary constraint $a = b^2/(4c) > 0$ in (11). For the plots, $\alpha = 1$, $\beta = 6$, $\gamma = 1$, $b = 1$, $c = 1$, and the wave number $k = 2$ are used. As the strength of the nonlinear dispersion term ε is varied, the amplitude of $u(x,0)$ increases but that of $v(x,0)$ decreases.

of the auxiliary ordinary differential equation

$$\left(\frac{\mathrm{d}z}{\mathrm{d}\xi}\right)^2 = az^2(\xi) + bz^3(\xi) + cz^4(\xi), \tag{5}$$

where a, b, and c are real parameters. Then

$$z(\xi) = \begin{cases} \dfrac{-ab\,\mathrm{sech}^2(\pm\frac{\sqrt{a}}{2}\xi)}{b^2 - ac\,(1-\tanh(\pm\frac{\sqrt{a}}{2}\xi))^2} & \text{when } a > 0, \textit{ type I,} \\ \dfrac{2a\,\mathrm{sech}(\sqrt{a}\xi)}{\sqrt{b^2-4ac} - b\,\mathrm{sech}(\sqrt{a}\xi)} & \text{when } \sqrt{b^2-4ac} > 0 \\ & \text{and } a > 0, \textit{ type II,} \end{cases} \tag{6}$$

are the exact solutions of (5).

To look for the traveling wave solutions of (1) in particular, we make the transformations $u(x,t) = u(\xi)$ and $v(x,t) = v(\xi)$, leading to

$$\begin{aligned} &(\beta k u - \omega)u_\xi + \alpha k v v_\xi + \gamma k^3 u_{\xi\xi\xi} = 0, \\ &\delta k u_\xi v + (\delta k u - \omega + \varepsilon k v)v_\xi = 0. \end{aligned} \tag{7}$$

By balancing the highest order derivative term $u_{\xi\xi\xi}$ with the highest order nonlinear term uu_ξ, we find $n = 2$. Similarly, we find $m = 2$ from the balance of vv_ξ and uu_ξ in the second equation of (1). Thus, we use the ansatz (4) for (1) as

$$\begin{aligned} u(\xi) &= u_0 + u_1 z(\xi) + u_2 z(\xi)^2, \\ v(\xi) &= v_0 + v_1 z(\xi) + v_2 z(\xi)^2. \end{aligned} \tag{8}$$

By substituting (5) and (8) into (7) and setting the coefficients of $z^j(\xi)(j = 0,1,2,\ldots,7)$ to zero, we find a set of algebraic equations for u_i, v_i, a, b, c, k, and ω as

$$\begin{aligned}
&-u_1\omega + u_1\beta u_0 k + \gamma k^3 u_1 a + \alpha v_0 v_1 k = 0, \\
&-bu_1\omega + bu_1\beta u_0 k + 4b\gamma k^3 u_1 a + b\alpha v_0 v_1 k \\
&\quad + a\alpha k {v_1}^2 - 2au_2\omega + 2au_2\beta u_0 k + 2a\alpha k v_0 v_2 \\
&\quad + 8\gamma u_2 k^3 a^2 + a\beta {u_1}^2 k = 0, \\
&-cu_1\omega + cu_1\beta u_0 k + 7c\gamma k^3 u_1 a + c\alpha v_0 v_1 k \\
&\quad + 3\gamma k^3 u_1 b^2 + b\alpha k {v_1}^2 - 2bu_2\omega + 2bu_2\beta u_0 k \\
&\quad + 2b\alpha k v_0 v_2 + 23b\gamma u_2 k^3 a + b\beta {u_1}^2 k \\
&\quad + 3ak\alpha v_1 v_2 + 3ak\beta u_1 u_2 = 0, \\
&9c\gamma k^3 u_1 b + c\alpha k {v_1}^2 - 2cu_2\omega + 2cu_2\beta u_0 k \\
&\quad + 2c\alpha k v_0 v_2 + 32c\gamma u_2 k^3 a + c\beta {u_1}^2 k \\
&\quad + 15\gamma u_2 k^3 b^2 + 3bk\alpha v_1 v_2 + 3bk\beta u_1 u_2 \\
&\quad + 2ak\beta {u_2}^2 + 2ak\alpha {v_2}^2 = 0, \\
&k(6k^2\gamma u_1 c^2 + 39k^2 c\gamma u_2 b + 2{u_2}^2\beta b \\
&\quad + 3c\alpha v_1 v_2 + 3c\beta u_1 u_2 + 2b\alpha {v_2}^2) = 0, \\
&{u_2}^2\beta + 12ck^2\gamma u_2 + \alpha {v_2}^2 = 0, \\
&v_1\varepsilon v_0 k + \delta u_1 k v_0 - v_1\omega + v_1\delta u_0 k = 0, \\
&2av_2\delta u_0 k - 2av_2\omega + 2a\delta u_2 k v_0 + 2av_2\varepsilon v_0 k \\
&\quad + 2a\delta u_1 k v_1 + a{v_1}^2\varepsilon k + bv_1\varepsilon v_0 k + b\delta u_1 k v_0 \\
&\quad - bv_1\omega + bv_1\delta u_0 k = 0, \\
&3a\delta u_1 k v_2 + 3av_2\varepsilon v_1 k + 3a\delta u_2 k v_1 + 2bv_2\delta u_0 k \\
&\quad - 2bv_2\omega + 2b\delta u_2 k v_0 + 2bv_2\varepsilon v_0 k + 2b\delta u_1 k v_1 \\
&\quad + b{v_1}^2\varepsilon k + cv_1\varepsilon v_0 k + c\delta u_1 k v_0 - cv_1\omega \\
&\quad + cv_1\delta u_0 k = 0, \\
&4a\delta u_2 k v_2 + 2a{v_2}^2\varepsilon k + 3b\delta u_1 k v_2 + 3bv_2\varepsilon v_1 k \\
&\quad + 3b\delta u_2 k v_1 + 2cv_2\delta u_0 k - 2cv_2\omega + 2c\delta u_2 k v_0 \\
&\quad + 2cv_2\varepsilon v_0 k + 2c\delta u_1 k v_1 + c{v_1}^2\varepsilon k = 0,
\end{aligned}$$

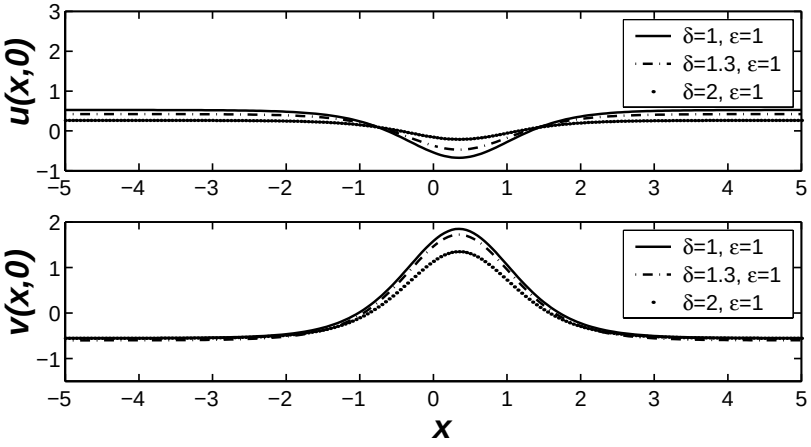

Fig. 2. The profiles of dark and bright solitary-waves $u(x,0)$ and $v(x,0)$, respectively. Due to negative third-order dispersion coefficient, i. e., $\gamma = -1$, the polarities of $u(x,0)$ and $v(x,0)$ are reversed in comparison with Figure 1. The parameters $b = -1$ and $c = 1$ are used to satisfy the auxiliary constraint $a = b^2/(4c) > 0$. For the plots, $\alpha = 1$, $\beta = 6$, $\gamma = -1$, $b = 1$, $c = 1$, and the wave number $k = 2$ are used. The amplitudes of both $u(x,0)$ and $v(x,0)$ increase as the strength of the combined nonlinear term, i. e., $\delta(uv)_x$, is increased.

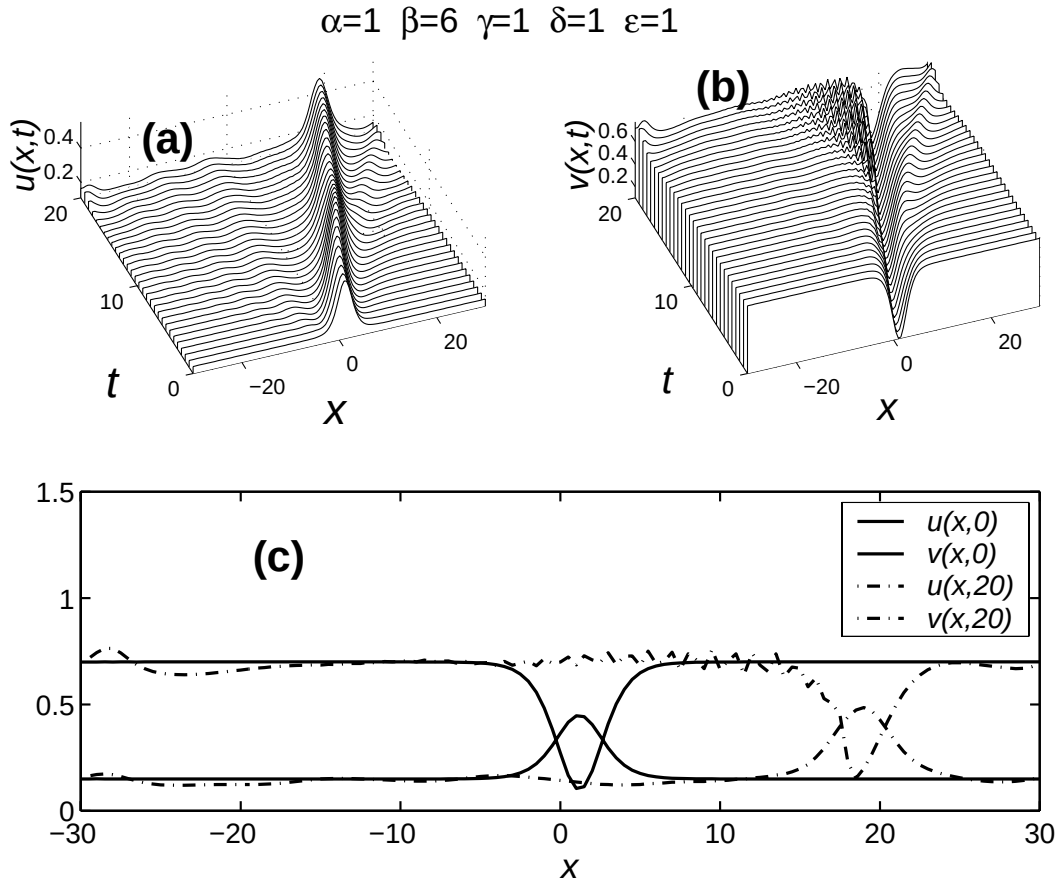

Fig. 3. (a), (b) Evolution of numerically simulated $u(x,t)$ and $v(x,t)$, respectively, with the initial profiles (15), the parameters $b = 1$ and $c = 1$, and the wave number $k = 1$. (c) Snap shots of the numerically simulated wave profiles at $t = 20$. Both the bright and dark solitary-waves emit radiation in form of an oscillating tail. Note that the velocities of the two solitary-waves are in phase.

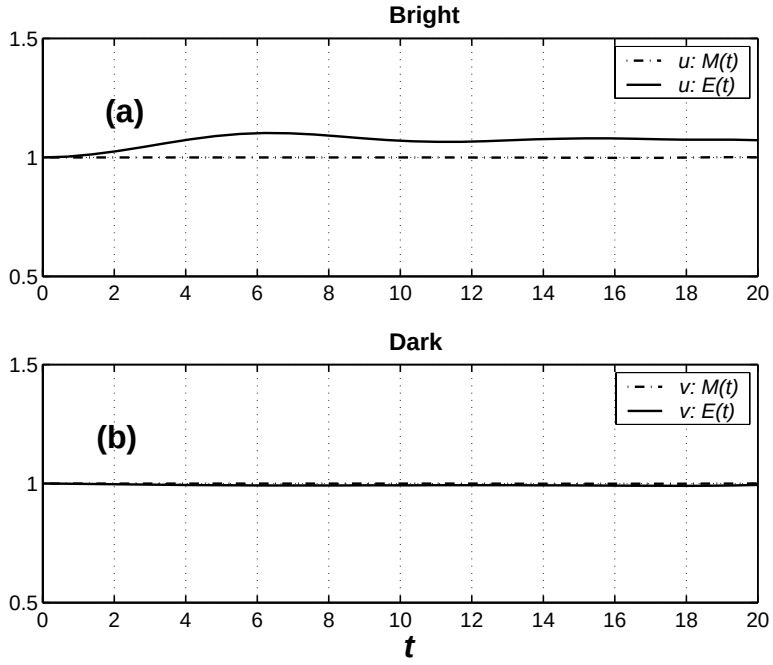

Fig. 4. (a) Evolution of the normalized mass and energy $M(t)$ and $E(t)$ for the bright solitary-wave $u(x,t)$ in Figure 3. $E(t)$ changes slightly during the evolution, while $M(t)$ does not deviate from its initial value. (b) Both the mass and energy of the dark solitary-wave $v(x,t)$ are conserved.

$$k(4b\delta u_2v_2+2b{v_2}^2\varepsilon+3c\delta u_1v_2+3cv_2\varepsilon v_1 +3c\delta u_2v_1)=0,$$

$$2cv_2k(2u_2\delta+v_2\varepsilon)=0. \quad (9)$$

We obtain the solution of the overdetermined set of algebraic equations in (9):

$$\begin{aligned} u_0&=\frac{\omega\varepsilon^2+4\alpha\delta\omega-\gamma k^3a\varepsilon^2}{(\beta\varepsilon^2+4\alpha\delta^2)k},\\ u_1&=-\frac{6\gamma k^2\varepsilon^2b}{\beta\varepsilon^2+4\alpha\delta^2},\ u_2=-\frac{12\gamma k^2c\varepsilon^2}{\beta\varepsilon^2+4\alpha\delta^2},\\ v_0&=\frac{2\varepsilon(-\delta\omega+\delta\gamma k^3a+\omega\beta)}{(\beta\varepsilon^2+4\alpha\delta^2)k},\\ v_1&=\frac{12\delta\gamma k^2\varepsilon b}{\beta\varepsilon^2+4\alpha\delta^2},\ v_2=\frac{24\gamma k^2c\varepsilon\delta}{\beta\varepsilon^2+4\alpha\delta^2}, \end{aligned} \quad (10)$$

under the constraint among a,b, and c as

$$b^2-4ac=0. \quad (11)$$

This condition in fact indicates that the solution set in (10) satisfies only the *type I* solution in (6), if, in conjunction with the constraint, $a=b^2/4c>0$, we require the parameter c to satisfy $c>0$. Upon substituting all this into (8), we find new analytic solitary-wave solutions of (1), with k and ω as free parameters, in the form

$$\begin{aligned} u(x,t)&=\frac{\omega\varepsilon^2+4\alpha\delta\omega-\gamma k^3a\varepsilon^2}{(\beta\varepsilon^2+4\alpha\delta^2)k}\\ &\quad+\frac{6\gamma k^2\varepsilon^2b}{\beta\varepsilon^2+4\alpha\delta^2}\Lambda(x,t)\\ &\quad-\frac{12\gamma k^2c\varepsilon^2}{\beta\varepsilon^2+4\alpha\delta^2}\Lambda(x,t)^2,\\ v(x,t)&=\frac{2\varepsilon(-\delta\omega+\delta\gamma k^3a+\omega\beta)}{(\beta\varepsilon^2+4\alpha\delta^2)k}\\ &\quad-\frac{12\delta\gamma k^2\varepsilon b}{\beta\varepsilon^2+4\alpha\delta^2}\Lambda(x,t)\\ &\quad+\frac{24\gamma k^2c\varepsilon\delta}{\beta\varepsilon^2+4\alpha\delta^2}\Lambda(x,t)^2, \end{aligned} \quad (12)$$

where

$$\Lambda(x,t)=\frac{ab\,\mathrm{sech}^2(\frac{\sqrt{a}}{2}(kx-\omega t))}{b^2-ac[1-\tanh(\frac{\sqrt{a}}{2}(kx-\omega t))]^2}. \quad (13)$$

Figures 1 and 2 show the profiles of the solitary-waves $u(x,0)$ and $v(x,0)$ in (12), respectively, for different model coefficients and a,b, and c satisfying (11). It is worth noting that, depending on the signs of the model coefficients, for example for $\gamma<0$, the polarities of $u(x,0)$ and $v(x,0)$ can be reversed, as shown in

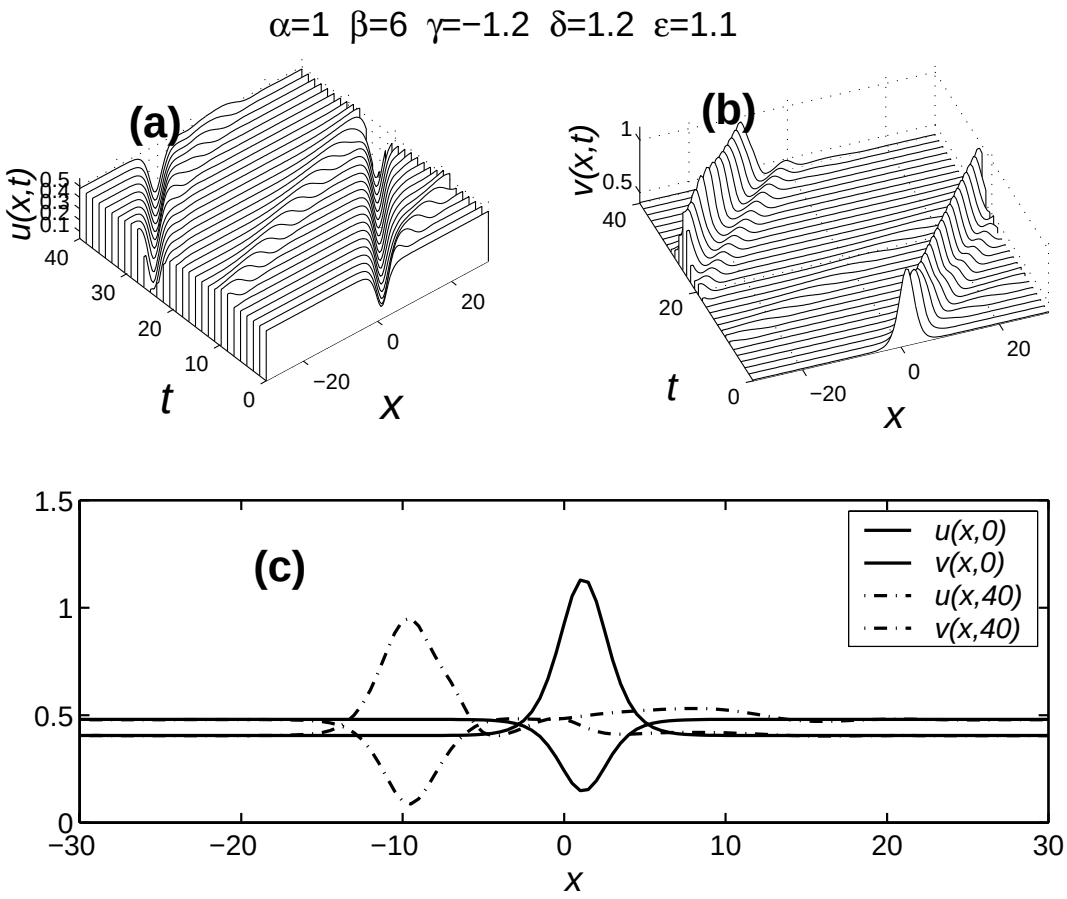

Fig. 5. Evolutions of the numerically simulated (a) dark solitary-waves $u(x,t)$, and (b) bright solitary-waves $v(x,t)$, with the initial profiles (15). Note the reversed polarities of the solitary-waves in comparison with Fig. 3, due to negative γ value. For the simulations, $b=1$ and $c=1$, and the wave number $k=1$ are used. (c) Snap shots of the numerically simulated wave profiles at $t=40$. The heights of both the bright and dark solitary-waves decrease and radiation in form of an oscillating front is emitted. Note that the velocities of the two solitary-waves are in phase.

Fig. 2, in comparsion with those in Figure 1. Figure 1 shows the effect of the nonlinear dispersion term ε on the amplitudes of the solitary-waves, i.e., the amplitude of $u(x,0)$ increases but that of $v(x,0)$ decreases if ε is increased. However, as shown in Fig. 2, the amplitudes of both $u(x,0)$ and $v(x,0)$ increase as the strength of the combined nonlinear term, i.e., $\delta(uv)_x$, is increased.

Finally, we note that the nonzero backgrounds at infinity, i. e., u_0 and v_0, can be made to zero by imposing special dispersion relations for u and v, as

$$u_0 = \frac{\omega\varepsilon^2 + 4\alpha\delta\omega - \gamma k^3 a\varepsilon^2}{(\beta\varepsilon^2 + 4\alpha\delta^2)k} = 0$$
$$\Longrightarrow \omega_u = \frac{\gamma a\varepsilon^2}{\varepsilon^2 + 4\alpha\delta}k^3,$$

$$v_0 = \frac{2\varepsilon(-\delta\omega + \delta\gamma k^3 a + \omega\beta)}{(\beta\varepsilon^2 + 4\alpha\delta^2)k} = 0$$
$$\Longrightarrow \omega_v = \frac{\delta\gamma a}{\delta - \beta}k^3. \tag{14}$$

However, in the following analysis we will investigate the dynamical properties of the solitary- waves in nonzero background, i.e, by using the solutions in (12) as the initial wave profiles.

3. Numerical Simulations

In this section we numerically integrate (1) to understand the stability and dynamics of the solitary-wave solutions discussed in Section 2. Here, "stability" means that the analytic solitary-wave preserves its

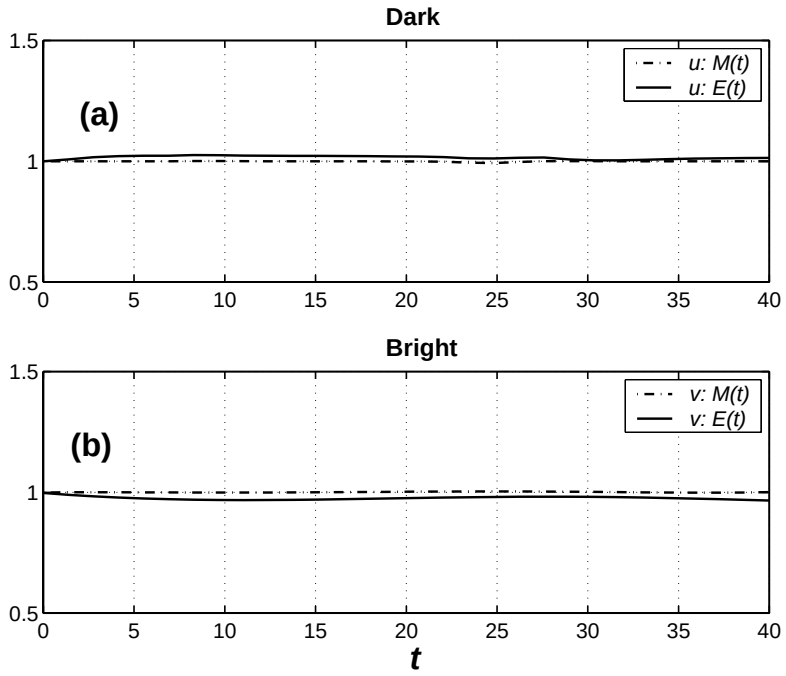

Fig. 6. Evolutions of the normalized mass and energy $M(t)$ and $E(t)$ for the (a) dark and (b) bright solitary-waves, respectively, as simulated in Fig. 5, which indicate their conservations. With negative third order dispersion $\gamma = -1.2$, more stable wave propagation is observed in comparison with the positive γ case in Figure 4.

initial profile, when it is substituted to (1) and numerically integrated for a long propagation time without losing its energy by radiation. The numerical scheme used in this work is based on the time advance using the Runge-Kutta fourth-order scheme and a pseudo-spectral method using the discrete fast Fourier transformation in the spatial discretization [8], applying periodic boundary conditions. The numerical errors in the spatial discretization were controlled by varying the number of discrete Fourier modes between 128 and 1024 and various time steps between 10^{-5} and 10^{-3}.

In the following, we first investigate the stability of the solitary-wave solutions by taking the initial profiles in the form

$$u(x,0) = \frac{6\gamma k^2\varepsilon^2 b}{\beta\,\varepsilon^2 + 4\,\alpha\,\delta^2}\Lambda(x) - \frac{12\gamma k^2 c\varepsilon^2}{\beta\,\varepsilon^2 + 4\,\alpha\,\delta^2}\Lambda(x)^2,$$
$$v(x,0) = -\frac{12\delta\,\gamma k^2\varepsilon\, b}{\beta\,\varepsilon^2 + 4\,\alpha\,\delta^2}\Lambda(x) + \frac{24\gamma k^2 c\varepsilon\,\delta}{\beta\,\varepsilon^2 + 4\,\alpha\,\delta^2}\Lambda(x)^2, \tag{15}$$

where

$$\Lambda(x) = \frac{ab\,\mathrm{sech}^2(\frac{\sqrt{a}}{2}(kx))}{b^2 - ac\,[1-\tanh(\frac{\sqrt{a}}{2}(kx))]^2}. \tag{16}$$

Before proceeding, we note that (1) is in general a non-integrable equation, because it is not certain whether (1) contains infinite numbers of time-independent integrals. However, as at least the fundamental solitary-wave solutions indeed exist, we want to define the simplest two such integrals, namely, the normalized mass and energy, as

$$M(t) = \int_{-\infty}^{\infty} v(x,t)\mathrm{d}x \Big/ \int_{-\infty}^{\infty} v(x,0)\mathrm{d}x \tag{17}$$

and

$$E(t) = \int_{-\infty}^{\infty} v(x,t)^2\mathrm{d}x \Big/ \int_{-\infty}^{\infty} v(x,0)^2\mathrm{d}x, \tag{18}$$

to further understand the dynamics of the waves.

Figures 3a and b show the evolutions of the bright and dark solitary-waves $u(x,t)$ and $v(x,t)$, respectively, for the coefficients used in Figure 1. The bright solitary-wave becomes slightly unstable by emitting radiation in the form of an oscillatory tail, and the width of the wave spreads, as shown in Fig. 3c, while the dark solitary-wave maintains its initial shape up to $t \approx 10$, after which it also radiates. Interestingly, as calculated in Figs. 4a and b, the normalized mass $M(t)$ does not deviate from its initial values for both the bright and the dark solitary-waves. However, the normalized energy of the bright solitary-wave $E(t)$ in Fig. 4a shows a variation from its initial value, due

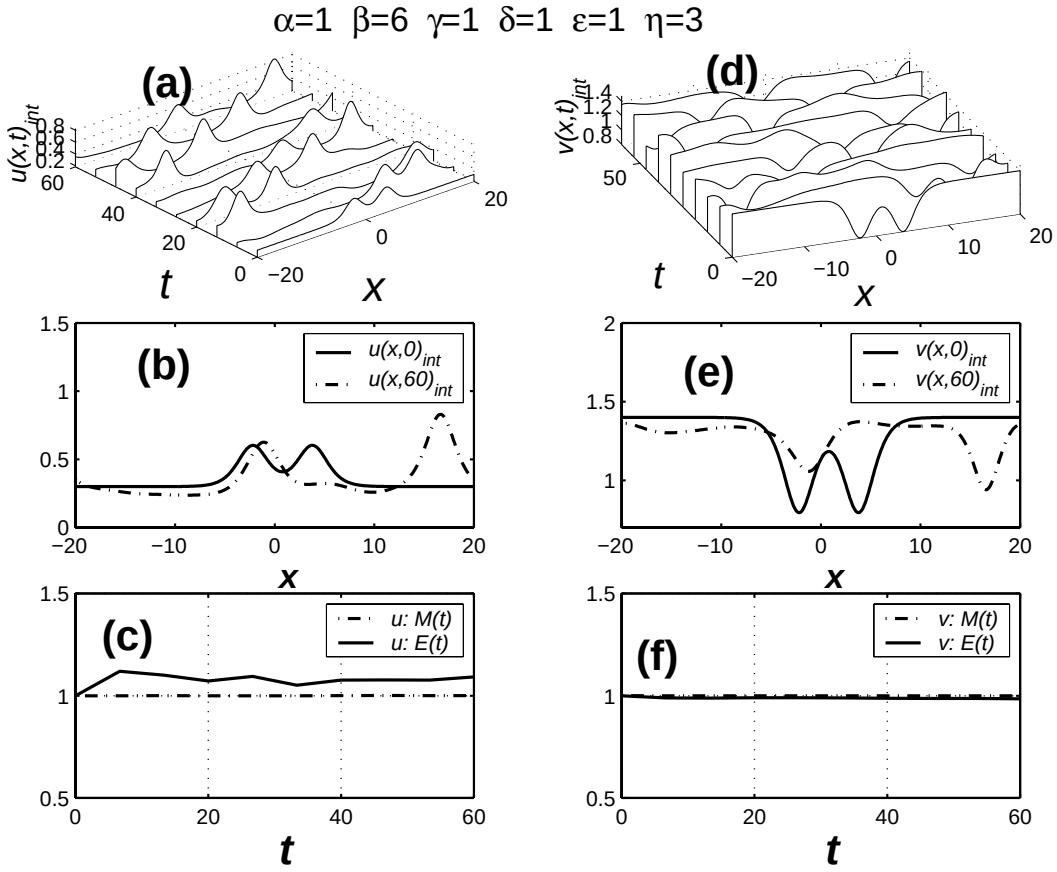

Fig. 7. Interaction dynamics of two solitary-waves with the initial profiles in (19), where the separation is $\eta = 3$. (a), (d) Evolutions of initially combined two bright and dark solitary-waves, respectively. (b), (e) Snap shots of the numerically simulated wave profiles at $t = 60$. The separation between the two solitary-waves increases and two bright solitary-waves with different amplitudes appear in (b). Similar behavior is observed for the dark solitary-waves in (e). (c), (f) While $M(t)$ for the bright and dark solitary-waves is conserved, the energy of the bright solitary-waves slightly increases, but the energy of the dark solitary-waves is conserved.

to the wave-width spreading and the radiation emission, while the energy of the dark solitary-wave is conserved as shown in Fig. 4b, in spite of the oscillatory nature of radiation in the tail. From these observations we conclude that the solitary-waves for the model coefficients are marginally unstable due to radiation loss during their propagation.

In Fig. 5, we simulate the evolutions of the bright and dark solitary-waves of the reversed polarities, i.e., $\gamma \to -\gamma$, but keeping the same coefficients as in Figure 3. In comparison with those in Fig. 3, the solitary-waves are more stable and the radiation in the oscillatory tail is less conspicuous during a longer propagation time, which is clearly demonstrated in Fig. 6, where $M(t)$ and $E(t)$ for both waves maintain their initial values. As it is expected, the velocities of the bright and dark solitary-waves are in phase, as depicted in Fig. 6c, since we set $k = 1$ and $\omega = 1$ for both waves. Though not presented here, we have confirmed by further numerical simulations that so long as the third-order dispersion term is negative ($\gamma < 0$), both the bright and dark solitary-waves are stable, regardless of the strength of the higher order nonlinear terms, i. e., $\delta(uu)_x$ and $\varepsilon v v_x$.

We now would like to understand the interaction dynamics of the bright and dark solitary-waves with the initial profiles

$$\begin{aligned} u(x,0)_{\text{int}} &= u(x+\eta) + u(x-\eta), \\ v(x,0)_{\text{int}} &= v(x+\eta) + v(x-\eta) \end{aligned} \tag{19}$$

where η is the separation between the solitary-waves. By using as an example the same set of coefficients

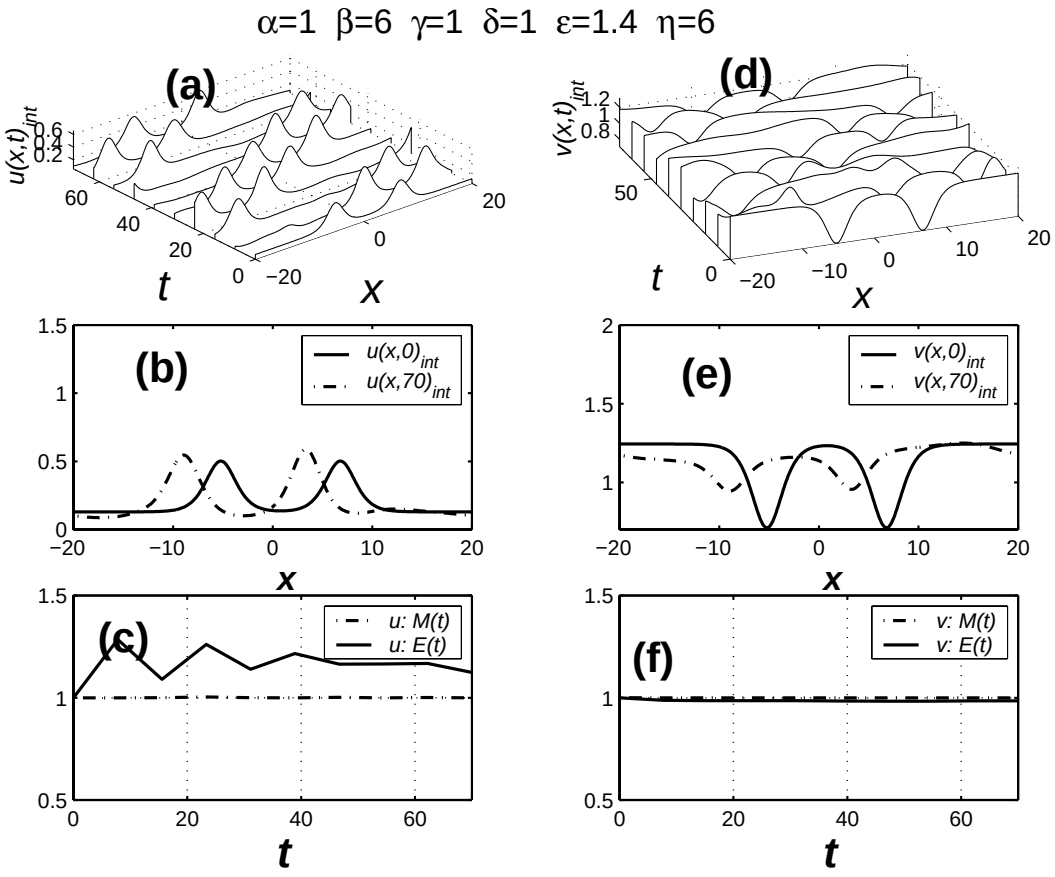

Fig. 8. Interaction dynamics of two solitary-waves with the initial profiles in (19), where the separation is $\eta = 6$. (a), (d) Evolutions of initially combined two bright and dark solitary-waves, respectively. (b), (e) Snap shots of the numerically simulated wave profiles at $t = 70$. The initial separation distance between the two bright solitary-waves is maintained in (b). Similar behavior is observed for the dark solitary-waves in (e). (c), (f) While $M(t)$ for the bright and dark solitary-waves is conserved, the energy of the bright solitary-waves slightly increases, but the energy for the dark solitary-waves is conserved.

as in Fig. 3, the interaction dynamics of the solitary-waves separated by $\eta = 3$ is simulated in Figure 7. Due to the short separation distance, the two bright solitary-waves in Fig. 7a are initially combined, however their interaction results in an increase of the separation distance between the waves, increase of the leading wave's amplitude, and oscillatory radiation in the tail, as shown in Fig. 7b for $t = 60$. Figure 7c shows the conservation of the normalized mass but a slight increase of $E(t)$ due to a weak instability, which may come from the unbalance between the dispersion and nonlinear terms in (1). Similar dynamical behaviors of the interacting two dark solitary-waves are observed in Figsures 7d – f. Even in the presence of the oscillatory radiation, it shows that the normalized mass and energy are conserved. This stability may come from the balance of the nonlinear terms, i. e., δ and ε in (1). After many simulations with different sets of coefficients, by fixing $\alpha = 1$ and $\beta = 6$ but varying $-1.2 < \gamma < -1.0$ and $1.0 < \delta$, $\varepsilon < 1.4$, we find a very similar dynamical behavior, as in Figure 7. Finally, we simulate the effect of the separation distance and larger nonlinear dispersion η on the interaction of the solitary-waves in Fig. 8, by using the same coefficients as in Fig. 7, but $\eta = 6$ and $\varepsilon = 1.4$. It is clearly demonstrated in Figs. 5c and e that at larger separation distance both the bright and dark solitary-waves evolve without any interaction. However, in comparision with Fig. 3a, the two bright solitary-waves separated by $\eta = 6$ are more stable during the propagation time.

4. Conclusions

In this work, we have found new analytic solitary-waves, having nonzero background at infinity, of the coupled Korteweg-De Vries equations [1 – 3], by utilizing the auxiliary equation method [6, 7]. It is shown that the nonzero background can be removed by imposing special dispersion relations as shown in (14). The bright and dark solitary-wave solutions in (12) exist under the constraints $a > 0$ and $b^2 - 4ac = 0$, and their polarities depend on the sign of the third-order dispersion term γ in (1). We have shown by numerical simulations the dynamics of the bright and dark solitary-waves in Figs. 3 and 5, and the evolution of the normalized mass and energy in Figs. 4 and 6. Depending on the sign of the third-order dispersion term, it has been demonstrated that the waves can be stable or unstable during their evolutions, as shown in Figures 3 – 6. By taking the two stable solitary-waves as initial profiles, as an example, we have simulated the interaction dynamics of the waves separated by $\eta = 3$ in Fig. 7, where the interactions result in an increase of the separation distance between the waves, increase of the leading wave's amplitude, and oscillatory radiation in the tail. However, more stable propagations are observed in the context of the mass and energy conservations. Finally, in Fig. 8, it has been demonstrated that at larger separation distance the solitary-waves maintain their initial profiles along the propagation distance.

Acknowledgement

This research was supported by the Catholic University of Daegu in 2005.

[1] C. Guha-Roy, J. Math. Phys. **28**, 2087 (1987).
[2] B. Lu, Z. Pan, B. Qu, and X. Jiang, Phys. Lett. A **180**, 61 (1993).
[3] B. Tian and Y. T. Gao, Int. J. Mod. Phys. **C12**, 361 (2001).
[4] C. Gu (ed.), Soliton Theory and its Application, Zhejiang Sci. Tech. Press, Hangzhou 1990.
[5] M. Ablowitz, P. A. Clarkson, and N. J. Hitchin, Soliton, Nonlinear Evolution Equations and Inverse Scattering, Cambridge University Press, Cambridge 1991.
[6] E. V. Krishnan, J. Math. Phys. **31**, 1155 (1990).
[7] E. Yomba, Chaos, Solitons and Fractals **21**, 75 (2004).
[8] L. N. Trefethen, Spectral Method in Matlab, Society for Industrial and Applied Mathemathics (Siam), Philadelphia, PA 2000.